JVI Journals.ASM.org

HIV-1 Replication and APOBEC3 Antiviral Activity Are Not Regulated by P Bodies

Prabhjeet K. Phalora,[a] Nathan M. Sherer,[a]* Steven M. Wolinsky,[b] Chad M. Swanson,[a] and Michael H. Malim[a]

Department of Infectious Diseases, Kings College London School of Medicine, Guy's Hospital, London, United Kingdom,[a] and Division of Infectious Diseases, Feinberg School of Medicine, Northwestern University, Chicago, Illinois, USA[b]

The APOBEC3 cytidine deaminases play a critical role in host-mediated defense against exogenous viruses, most notably, human immunodeficiency virus type-1 (HIV-1) and endogenous transposable elements. APOBEC3G and APOBEC3F interact with numerous proteins that regulate cellular RNA metabolism, including components of the RNA-induced silencing complex (RISC), and colocalize with a subset of these proteins to mRNA processing bodies (P bodies), which are sites of mRNA translational repression and decay. We sought to determine the role of P bodies and associated proteins in HIV-1 replication and APOBEC3 antiviral activity. While we established a positive correlation between APOBEC3 protein incorporation into virions and localization to P bodies, depletion of the P-body components DDX6 or Lsm1 did not affect HIV-1 replication, APOBEC3 packaging into virions or APOBEC3 protein mediated inhibition of HIV-1 infectivity. In addition, neither HIV-1 genomic RNA nor Gag colocalized with P-body proteins. However, simultaneous depletion of multiple Argonaute family members, the effector proteins of RISC, could modestly increase viral infectivity. Because some APOBEC3 proteins interact with several Argonaute proteins, we also tested whether they could modulate microRNA (miRNA) activity. We found no evidence for the specific regulation of miRNA function by the APOBEC3 proteins, though more general effects on transfected gene expression were observed. In sum, our results indicate that P bodies and certain associated proteins do not regulate HIV-1 replication or APOBEC3 protein antiviral activity. Localization to P bodies may therefore provide a means of sequestering APOBEC3 enzymatic activity away from cellular DNA or may be linked to as yet unidentified cellular functions.

The APOBEC3 (apolipoprotein B mRNA editing enzyme catalytic polypeptide-like 3) family of cytidine deaminases provides an innate mechanism of antiviral defense against a diverse range of exogenous viruses and endogenous retroelements (20, 67). The human APOBEC3 family consists of seven proteins; APOBEC3A (A3A), APOBEC3B (A3B), APOBEC3C (A3C), APOBEC3D/E (A3D/E), APOBEC3F (A3F), APOBEC3G (A3G), and APOBEC3H (A3H) (53). At least four members (APOBEC3D/E, APOBEC3F, APOBEC3G, and APOBEC3H) have anti-HIV-1 activity and are counteracted by the viral Vif protein (11, 28, 48, 81, 90, 99). In the absence of Vif, antiviral APOBEC3 proteins are incorporated into assembling virions and, following infection of the target cell, mediate deamination of cytidine residues to uridines in (mostly) nascent minus-strand reverse transcripts. These are detected as G-to-A mutations in the plus-strand viral DNA, and excessive editing, known as hypermutation, leads to loss of sequence integrity and the production of genetically compromised virions (40, 68, 69, 106). Editing-independent effects also contribute to HIV-1 inhibition, as A3F and A3G can impede reverse transcription in target cells (10, 12, 42, 43, 51). Vif prevents these proteins from being packaged by recruiting them to a cullin5-elonginB/C-Rbx2-CBFβ E3 ubiquitin ligase complex, resulting in their polyubiquitination and subsequent proteasomal degradation (24, 52, 69, 72, 104, 107).

A3F and A3G interact, mostly via RNA bridging, with a large number of RNA binding proteins that regulate mRNA metabolism, translation, and degradation and localize to discrete, nonmembraned structures termed processing bodies (P bodies) (21, 36, 37, 57, 98). These foci are concentrated sites of translationally repressed mRNAs and mRNA decay machinery, including the Dcp1a/Dcp2 decapping complex, the decapping coactivators DDX6 and Lsm1, and the 5′-3′ exoribonuclease Xrn1 (25, 83, 91). The Argonaute proteins also localize to P bodies and interact with A3F and A3G in a partially RNase-insensitive manner, suggestive of close and potentially direct interactions (36, 37). These proteins play a fundamental role in the process of RNA interference (RNAi), as they are the effector components of the RNA-induced silencing complex (RISC), which mediates translational repression and mRNA decay via microRNAs (miRNAs) and small interfering RNAs (siRNAs) (32, 50, 94).

There is increasing evidence to suggest that P-body and RISC proteins can influence diverse viral life cycles and may act as cofactors for the replication of certain viruses (7). Hepatitis C virus requires the miR-122 miRNA as well as the DDX6, Lsm1, and PatL1 proteins for viral protein expression and replication (54, 89). DDX6 also facilitates infectious virion production of the retrovirus primate foamy virus (PFV) (103). In the yeast *Saccharomyces cerevisiae*, virus-like particle formation and retrotransposition of the Ty1 and Ty3 retrotransposons are dependent upon the P-body components Dhh1p/DDX6, Lsm1p, and PatL1p (8, 18, 31). Similarly, several P-body proteins promote the translation

Received 7 March 2012 **Accepted** 10 August 2012

Published ahead of print 22 August 2012

Address correspondence to Chad M. Swanson, chad.swanson@kcl.ac.uk, or Michael H. Malim, michael.malim@kcl.ac.uk.

* Present address: Nathan M. Sherer, Institute for Molecular Virology and McCardle Laboratory for Cancer Research, University of Wisconsin—Madison, Madison, Wisconsin, USA.

Supplemental material for this article may be found at http://jvi.asm.org/.

doi:10.1128/JVI.00595-12

and replication of the plant RNA virus brome mosaic virus (BMV) (6, 29, 71, 80). Conversely, P-body components have also been shown to be inhibitory to some viruses and retroelements. Poliovirus infection causes disruption of P bodies and the specific degradation of Dcp1a and Xrn1 (30), and replication of PFV is restricted by the cellular miRNA miR-32 (59). In mice, inhibition of miRNA biogenesis, accomplished through knockdown of Dicer, increases the transcript abundance of intracisternal A particle (IAP) and murine endogenous retrovirus-L (MuERV-L) retrotransposons (93), and depletion of the P-body components DDX6 and eIF4E-T also increases IAP retrotransposition events (65).

A number of reports have indicated that HIV-1 has substantial interactions with miRNA and P-body-associated proteins. HIV-1 infection has been shown to modulate cellular miRNA production (41, 44, 101), and both cellular miRNAs targeting HIV-1 and putative virally derived miRNAs have been identified by some groups (2, 47, 56, 73, 82, 95), but not others (61, 84). Two groups have reported that siRNA-mediated knockdown of RISC and P-body-associated proteins results in increased virus production and/or infectivity, with both studies also suggesting that HIV-1 RNA localizes to P bodies (17, 73). In contrast, more recent reports have found that Argonaute 2 (Ago2) or DDX6 depletion decreases HIV-1 production by 50 to 80%, (13, 86), highlighting the controversial role that P-body proteins play in HIV-1 replication.

Why certain APOBEC3 proteins localize to and interact with P-body and RISC components remains unresolved. It is plausible that these complexes or specific associated proteins may promote APOBEC3 protein packaging into virions, thereby acting as cofactors for APOBEC3-mediated HIV-1 restriction. Recently, APOBEC3 antiviral activity has been positively correlated with virion incorporation (48), but it remains unclear as to exactly what cellular or viral factors are required for packaging. A3G virion incorporation is dependent upon its interaction with the nucleocapsid region of Gag (16, 74, 88), but the identity of the RNA(s) that bridges this interaction remains controversial (55). It has been proposed, for instance, that APOBEC3 proteins are packaged in association with polymerase III (Pol III) RNAs, which are themselves incorporated into virions (97). However, we previously reported that A3F does not detectably interact with these RNAs, even though it is efficiently incorporated into HIV-1 particles (36, 49). Alternatively, APOBEC3 localization to P bodies may be indicative of cellular functions that are distinct from viral inhibition, potentially concerning the control of cellular mRNA expression. In particular, the closely related family member APOBEC1 is able to bind to and stabilize several AU-rich element (ARE)-containing mRNAs (3, 4, 19), and the APOBEC3 proteins themselves have been reported to inhibit miRNA-mediated translational repression (46). Very recently, this inhibition has been attributed to competition between A3G and Ago2 for binding to the RISC and P-body component MOV10 (62). Therefore, a subset of APOBEC3 proteins may localize to P bodies and interact with the miRNA machinery to regulate cellular mRNAs.

In this study, we aimed to determine the role of P bodies and associated proteins in APOBEC3 protein activity. We established a positive correlation between localization to P bodies and packaging into viral particles and hence sought to determine the influence of these foci on APOBEC3-mediated HIV-1 inhibition and virion incorporation as well as on HIV-1 replication in general. We also identified several APOBEC3 proteins, in addition to A3F and A3G, which interact with Ago2 and hence explored the functional significance of this interaction with regard to a role of the APOBEC3 proteins as regulators of cellular mRNA translation through miRNA inhibition.

MATERIALS AND METHODS

Expression vectors and RNA silencing. All plasmid manipulations were performed using standard PCR-based methods, and all constructs were confirmed to be correct by sequencing and restriction digest. The carboxyl-terminal hemagglutinin (HA)-tagged human APOBEC3 (A, B, C, F, and G) expression vectors have previously been described (11). cDNAs encoding APOBEC3D/E, APOBEC3H (haplotype II), or green fluorescent protein (GFP) were inserted into the same vector using the HindIII and XbaI restriction sites. cDNA encoding firefly luciferase (pLuc), with a stop codon at the end of the open reading frame to prevent expression of the HA tag, was also inserted into this vector using the Asp718 and HindIII restriction sites. A3G or yellow fluorescent protein (YFP) was cloned into the retroviral vector pNG/neo (90) by insertion using either the EcoRI and NotI or EcoRI and BglII sites to give pNG/neo/A3G and pNG/neo/YFP, respectively. Amino-terminal Myc-tagged DDX6 was constructed by inserting the DDX6 cDNA into the pcDNA3.1-myc expression vector (63) using the BamHI and XhoI restriction sites to generate pMyc-DDX6. The NL4-3 Δ*vif* proviral plasmid ($pHIV_{NL4\text{-}3\Delta vif}$) was generated by introducing two stop codons into the *vif* reading frame of $pHIV_{NL4\text{-}3}$ (1) by overlapping PCR. The NL4-3 protease-deficient derivative ($pHIV_{NL4\text{-}3/Pr\text{-}}$) was a kind gift from E. Freed (45a). The NL4-3 proviral plasmid containing 24 binding loops from the MS2 bacteriophage ($pHIV_{NL4\text{-}3/24\times MS2}$) was generated by insertion of the SacII and BsmB1 restriction sites at the end of the *gag* reading frame in the parental pNL4-3 expression plasmid by overlapping PCR to give $pHIV_{NL4\text{-}3/SB}$. The 24 MS2 binding loops (35) were then directly subcloned into $pHIV_{NL4\text{-}3/SB}$ using the SacII and BsmB1 sites to give $pHIV_{NL4\text{-}3/24\times MS2}$. Plasmids encoding 24 MS2 binding loops and MS2-YFP were kind gifts from R. Singer (35). The proviral plasmid construct that contained Gag fused to the Venus fluorescent protein ($pHIV_{NL4\text{-}3/Gag\text{-}Venus}$) was a kind gift from A. Ono (22). pcDNA3.1 plasmids encoding Myc-tagged Ago1, Ago2, and Ago3 were kindly provided by G. Hannon (63). The luciferase reporter constructs FF4LCS (wild type) and FF4rmLCS (mutant) were a kind gift from J. Steitz (66). The TK/*Renilla* plasmid (pGL4.74) was purchased from Promega. The vesicular stomatitis virus G (VSV-G) protein expression vector has previously been described (34). The short hairpin RNA (shRNA) lentiviral vectors were obtained from Open Biosystems (pGIPZ shRNAmir-GFP; Ago2/V2LHS_241069, DDX6/V2LHS_23998, Lsm1/V2LHS_213130). The Argonaute and DDX6 siRNA oligonucleotides were from Ambion Life Technologies (*Silencer* Select siRNA; Ago1/s25501, Ago2/s25932, Ago3/s46948, Ago4/s46949, DDX6/s4012). The ALIX siRNA oligonucleotide has previously been described (15).

Cell culture and stable cell lines. 293T, HeLa, and TZM-bl cells were cultured in Dulbecco modified Eagle medium, and HUT78 cells were cultured in RPMI supplemented with 10% fetal bovine serum plus penicillin-streptomycin. HeLa cells stably expressing A3G or YFP were produced by standard retrovirus-mediated transduction using pNG/neo/A3G or pNG/neo/YFP, respectively, and selection with G418 (0.5 mg/ml). Cell lines stably expressing either a nonsilencing control, Ago2, DDX6, or Lsm1 targeting shRNA were generated by standard lentivirus-mediated transduction and selection with puromycin (1 μg/ml). For shRNA- and DDX6 or ALIX siRNA-treated cells, protein expression and knockdown were confirmed by immunoblotting using either an anti-Ago2 (1/1,000; rat monoclonal 11A9; Sigma), anti-ALIX (1/10,000; rabbit polyclonal) (33), anti-DDX6 (1/3,000; rabbit polyclonal; Cambridge Biosciences), or anti-Lsm1 (1/500; chicken polyclonal; Sigma) antibody. For Argonaute siRNA-treated cells, RNA levels were determined by quantitative PCR (qPCR) analysis using TaqMan gene expression assays (Ago1/Hs01084653, Ago2/Hs01085579, Ago3/Hs01087121, Ago4/Hs01059731; Applied Biosystems).

Single-cycle infectivity assays. Subconfluent monolayers of 293T cells seeded in 35-mm plates were cotransfected with 0.5 μg of $pHIV_{NL4-3\Delta vif}$ and between 0.02 μg and 1.5 μg of pHA-APOBEC3A to APOBEC3H expression vectors using polyethylenimine (PEI). Forty-eight hours later, supernatants were harvested and virus levels were quantified by $p24^{Gag}$ enzyme-linked immunosorbent assay (ELISA; Perkin-Elmer). Virus equivalent to 5 ng $p24^{Gag}$ was used to challenge 10^5 TZM-bl indicator cells. At approximately 30 h postinfection, whole-cell lysates were assayed for the induction of β-galactosidase expression using a Galacto-Star system (Applied Biosystems).

Virion incorporation assays. Virus equivalent to 20 ng $p24^{Gag}$ was purified through a 20% (wt/vol) sucrose cushion at 21,000 × *g* for 2 h at 4°C. Viral pellets were resuspended in loading buffer (60 mM Tris-HCl [pH 6.8], 0.1 M DL-dithiothreitol [DDT], 10% glycerol, 2% sodium dodecyl sulfate [SDS], 0.1% bromophenol blue) and analyzed by immunoblotting. Whole-cell lysates from the corresponding virus producer cells were analyzed in parallel. A3G virion incorporation was also assessed by immunoblot analysis using an anti-A3G antibody (1/1,000; rabbit polyclonal) (76).

Virus infections and replication. Subconfluent monolayers of HeLa cells seeded in 35-mm cultures were infected with 293T cell-generated VSV-G-pseudotyped HIV_{NL4-3} or $HIV_{NL4-3\Delta vif}$ equivalent to 50 ng $p24^{Gag}$. Four hours later, input virus was removed and cells were thoroughly washed before the addition of fresh medium. At 48 h postinfection, supernatants were harvested and viral infectivity was measured by a single-cycle infectivity assay.

Approximately 3×10^6 HUT78 cells were infected with HIV_{NL4-3} or $HIV_{NL4-3\Delta vif}$ equivalent to 5 ng, 25 ng, or 125 ng $p24^{Gag}$. Two hours later, input virus was removed and cells were thoroughly washed before the addition of fresh medium. Every 2 days postinfection, 5 ml of culture medium was collected (and replaced with fresh medium) and centrifuged at 500 × *g* for 5 min. The supernatant was harvested for quantification by $p24^{Gag}$ ELISA, and cell pellets were resuspended in loading buffer for determination of protein expression by immunoblot analysis.

HIV-1 genome incorporation assays. Subconfluent layers of 293T cells were cotransfected with equivalent amounts of $pHIV_{NL4-3/24\times MS2}$ or $pHIV_{NL4-3/Pr-}$ and either the Gag-Pol plasmid p8.91 or the luciferase-encoding expression plasmid pLuc. Forty-eight hours later, viral supernatants were harvested and treated with 20 U/ml RQ1 DNase (Promega) in 10 mM $MgCl_2$ for 3 h at 37°C, prior to sucrose cushion purification. Viral pellets were subject to RNA extraction using an miRNeasy kit (Qiagen). cDNA was synthesized using a high-capacity cDNA archive kit (Applied Biosystems) with 50 ng of extracted RNA. qPCRs were performed as previously described (39), using primers oNS172f (5′-GGCCAGGGAATTT TCTTCAGA) and oNS173r (5′-TTGTCTCTTCCCCAAACCTGA) and probe oNS174p (5′–6-carboxyfluorescein [FAM]–ACCAGAGCCAA-CAGCCCCACCAGA–6-carboxytetramethylrhodamine [TAMRA]).

Coimmunoprecipitation. Subconfluent monolayers of 293T cells, in 35-mm cultures, were cotransfected with 2 μg of HA-tagged APOBEC3 expression vectors (pHA-APOBEC3A to pHA-APOBEC3H and 2 μg of pMyc-Argonaute 1 to Argonaute 3 expression plasmids. Forty-eight hours later, cells were harvested in phosphate-buffered saline (PBS) and pelleted at 500 × *g* for 5 min. Cell pellets were resuspended in 0.05% HCHO and incubated at 37°C for 10 min. Cells were washed in PBS and resuspended in 0.25 M glycine for 5 min at room temperature. Cells were washed in PBS and resuspended in 1× BB lysis buffer (0.5% NP-40, 150 mM KCl, 10 mM HEPES [pH 7.0], 6 mM $MgCl_2$, 2 mM DDT, 10% glycerol, and complete protease inhibitor cocktail [Roche]) for 10 min on ice. Lysates were sonicated (3 times for 10 s) before being cleared by centrifugation for 10 min at 1,000 × *g*. Protein G agarose (Invitrogen) was preincubated with an anti-Myc (1/1,000; mouse monoclonal 9E10) antibody for 1 h 30 min at 4°C and then mixed with lysate for 2 h at 4°C on a rotational tumbler. Samples were washed 5 times in 1× radioimmunoprecipitation assay buffer (10 mM Tris-HCl [pH 7.5], 150 mM NaCl, 1 mM EDTA, 0.1% SDS, 1% Triton X-100, 1% sodium deoxycholate) and resuspended in reverse cross-linking buffer (10 mM EDTA, 5 mM DDT, 0.5% SDS) for 45 min at 65°C before eluting in loading buffer. Samples were analyzed by SDS-PAGE using 10% gels for APOBEC3 proteins and 7% gels for Argonaute proteins. Resolved proteins were detected by immunoblotting using anti-HA (1/1,000; rabbit polyclonal; Rocklands) or anti-Myc (1/1,000) antibodies. Bound antibodies were visualized either by appropriate horseradish peroxidase-conjugated secondary antibodies (1/3,000; Pierce) and enhanced chemiluminescence or by infrared IRDye-conjugated secondary antibodies (1/5,000; LI-COR Biosciences) and LI-COR infrared imaging technology (LI-COR UK Ltd.).

Immunofluorescence. HeLa or 293T cell monolayers (10^5 cells) were directly seeded onto 13-mm glass coverslips. For nonadherent HUT78 cells, coverslips were first treated with poly-L-lysine (Sigma) as per the manufacturer's instructions and dried overnight. Twenty-four hours later, cells were washed three times in PBS and fixed with 4% paraformaldehyde (Electron Microscopy Sciences) for 15 min. Cells were washed again, permeabilized with 0.2% Triton X-100 for 12 min at room temperature, and then simultaneously blocked and quenched with NGB buffer (50 mM NH_4Cl, 1% goat serum, 1% bovine serum albumin) for 1 h. For P-body detection, cells were first incubated with either an anti-DDX6 (1/500) or an anti-Ge1 (1/500; mouse monoclonal; Santa Cruz) antibody for 2 h. Cells were washed and incubated with the appropriate species-specific Alexa Fluor 488- or 594-conjugated secondary antibody (1/500; Molecular Probes) for 1 h. To visualize nuclei, cells were additionally incubated with 4′,6′-diamidino-2-phenylindole (DAPI) dilactate (1/25,000; Molecular Probes) for 1 min. Coverslips were mounted onto slides using Mowiol mounting medium (Calbiochem). Laser scanning confocal imaging was performed on a DM IRE2 microscope (Leica), and the images were processed using LCS (Leica), Openlab (Improvision), and Photoshop (Adobe) software packages.

For APOBEC3 and P-body localization studies, 10^5 HeLa cell monolayers seeded on 13-mm coverslips were cotransfected with 0.2 μg of pHA-APOBEC3(A-H) expression plasmids and 0.2 μg of pMyc-DDX6 or pMyc-Ago2 expression plasmids using Fugene 6 (Roche). At approximately 30 h posttransfection, cells were fixed and stained with anti-HA (1/500) and anti-Myc (1/500) primary antibodies and appropriate species-specific Alexa Fluor 488- or 594-conjugated secondary antibodies and DAPI. Coverslips were treated and analyzed by confocal microscopy, as described above.

For HIV-1 genomic RNA (gRNA) and P-body localization studies, 0.5 μg of the MS2-YFP expression vector was transfected alone or cotransfected with between 0.018 and 0.5 μg of the $pHIV_{NL4-3/24\times MS2}$ proviral expression plasmid. For $pHIV_{NL4-3/24\times MS2}$, expression of Pol is disrupted, and thus, some experiments were also performed with complementation using wild-type virus. For analysis of HIV-1 Gag and P-body localization, 0.5 μg of the $pHIV_{NL4-3/Gag-Venus}$ proviral plasmid was transfected into HeLa cells. pLuc was also included to keep total DNA concentrations equivalent for each transfection. At approximately 30 h posttransfection, cells were fixed and stained with an anti-GFP antibody (1/1,000; mouse monoclonal; Roche) to enhance the YFP signal (for MS2-YFP-containing samples) and either anti-DDX6 or anti-Ge1 antibodies for detection of P bodies and then appropriate species-specific Alexa Fluor 594-conjugated secondary antibodies and DAPI. Coverslips were treated and analyzed by confocal microscopy, as described above.

Luciferase reporter assays. HeLa cells plated at 10^5 cells in 24-well plates were cotransfected with 0.1 μg of firefly luciferase expression plasmid, 0.08 μg of *Renilla* luciferase expression plasmid, and 0.9 μg of pHA-APOBEC3(A-H) expression plasmids using Lipofectamine 2000 (Invitrogen). At 30 h posttransfection, cells were harvested and assayed using a dual-luciferase assay kit (Promega) as per the manufacturer's instructions.

RESULTS

Antiviral activities of the APOBEC3 proteins. The seven members of the APOBEC3 subfamily have various levels of antiviral

activity against different viral substrates (20, 26, 67). We directly compared the anti-HIV-1 phenotypes of all the APOBEC3 proteins in a single-cycle infectivity assay, using Δ*vif* viruses produced with the $pHIV_{NL4\text{-}3\Delta vif}$ provirus in the presence of HA-tagged APOBEC3 expression vectors [pHA-APOBEC3(A-H)]. Consistent with previous reports (11, 48, 60, 99, 105), A3G was the most potent member of this family, even at very low concentrations (see Fig. S1 in the supplemental material). The other APOBEC3 proteins showed a range of inhibitory phenotypes, from relatively strong (A3B, A3F, and A3H) to weak (A3A, A3C, and A3D/E) antiviral activity.

APOBEC3 virion incorporation correlates with P-body localization. Although not all of the APOBEC3 proteins are antiviral (see Fig. S1 in the supplemental material), they are all reportedly packaged into virions when ectopically expressed (27, 28, 38, 99, 102). In order to establish which APOBEC3 proteins can be detected in virions, 293T cells were cotransfected with pHA-APOBEC3(A-H) and $pHIV_{NL4\text{-}3\Delta vif}$ expression plasmids. Forty-eight hours later, supernatants were harvested and virions were purified through a 20% sucrose cushion (see Fig. S2A in the supplemental material). At a 1:3 ratio of APOBEC3 plasmid DNA to proviral plasmid DNA, A3G was clearly packaged with the highest efficiency, followed by A3F, A3H, and A3D/E.

To determine if APOBEC3 localization to P bodies (37, 77, 98) correlated with virion incorporation, HeLa cells were cotransfected with pHA-APOBEC3(A-H) and an expression vector for Myc-tagged DDX6 or Ago2, cellular proteins known to accumulate in P bodies. These cells were then analyzed by indirect immunofluorescence, and colocalization of APOBEC3 proteins with DDX6-marked (see Fig. S2B and C in the supplemental material) or Ago2-marked (see Fig. S3 in the supplemental material) foci was scored for 100 cells in each sample. A3DE, A3F, A3G, and A3H were found to localize with DDX6- and Ago2-marked P bodies in ~90% of cells. Thus, there appears to be a positive correlation between the localization of APOBEC3 proteins at P bodies and their incorporation into viral particles. It is important to note, however, that the proteins that most strongly associate with P bodies are also the ones that are predominantly cytoplasmic.

Role of P bodies in APOBEC3 antiviral activity and HIV-1 replication. As APOBEC3 protein localization to P bodies positively correlated with virion incorporation (see Fig. S2 and S3 in the supplemental material), we sought to investigate whether microscopically visible P bodies are necessary for infectious HIV-1 particle production and APOBEC3 antiviral activity. We first depleted P bodies from HeLa cells that stably express either A3G or YFP by transfecting an siRNA targeting the DDX6 mRNA. This led to the almost complete loss of P bodies from these cells, as observed by confocal microscopy (Fig. 1A and B) and a consistent reduction of DDX6 protein levels of between 80 and 90% compared to that for a cell line transfected with a nonsilencing control siRNA (Fig. 1E). Importantly, expression of another P-body protein, Lsm1, was unaffected by knockdown of DDX6, confirming the specificity of the silencing (data not shown).

All cell lines were then infected with wild-type or Δ*vif* HIV-1, corresponding to 50 ng $p24^{Gag}$, and 48 h later the abundance and infectivity of the virions in the media were analyzed by $p24^{Gag}$ ELISA and a single-cycle infectivity assay, respectively. Contrary to published findings (17, 73), we were unable to detect any increase in virus production (Fig. 1C) or HIV-1 infectivity (Fig. 1D) upon knockdown of DDX6 and depletion of visible P bodies. Further, DDX6 depletion did not affect the antiviral activity of A3G (Fig. 1D). Consistent with these findings, immunoblot analysis of purified virions demonstrated that there was no detectable difference in A3G packaging between the control and DDX6-knockdown cell lines (Fig. 1E). Equivalent results were obtained when HeLa cells were stably transduced with an shRNA-encoding lentiviral vector targeting DDX6 and a similar analysis was undertaken (data not shown). To verify these results further, we also depleted the P-body protein Lsm1 using lentiviral shRNA vectors. Analogous to knockdown of DDX6, depletion of Lsm1 led to a significant loss of visible P bodies and Lsm1 protein (~85%) (Fig. 2A, B, and E), but when the knockdown cell lines were infected with wild-type or Δ*vif* HIV-1, similar amounts of virus were produced, with no alteration in infectivity (Fig. 2C and D).

To determine if an effect of P-body depletion could be discerned over multiple rounds of viral replication, we then stably transduced HUT78 cells, a $CD4^+$ T cell line that naturally expresses anti-HIV-1 APOBEC3 proteins, including A3G, with either a nonsilencing control shRNA or an shRNA targeting Lsm1 mRNA. Transduction of HUT78 cells with the Lsm1 shRNA led to a substantial reduction in protein levels (~80%) and P bodies compared to control cells (Fig. 3A and B). Cells were then infected with wild-type or Δ*vif* virus, and spreading replication was monitored over several days (Fig. 3C). Knockdown of Lsm1 had no effect on HIV-1 replication, as there was no detectable difference between the two cell lines in terms of wild-type virus production. Furthermore, APOBEC3 protein-mediated antiviral activity was unaffected by loss of Lsm1, as observed by equivalent levels of suppression of the Δ*vif* virus in relation to the wild-type virus for both the control and knockdown cell lines. Knockdown of Lsm1 was maintained throughout the replication cycle (see Fig. S4A in the supplemental material), and similar results were observed, with virus inputs corresponding to 5 ng or 125 ng $p24^{Gag}$ (see Fig. S4B and C in the supplemental material). Therefore, both in single-cycle assays and in multiple rounds of replication, we found no effect of depletion of P-body proteins on HIV-1 virion production, infectivity, or A3G antiviral function.

Two groups have recently reported that knockdown of several P-body-associated proteins results in an increase in HIV-1 production and infectivity, utilizing either infection- or transfection-based experimental approaches (17, 73). In order to reconcile our results with published reports, we next tested whether depletion of DDX6 or Lsm1 affected virion production or infectivity when HeLa cells were transiently transfected with a proviral expression plasmid instead of being directly challenged with infectious virus. HeLa cells stably transduced with nonsilencing or DDX6- or Lsm1-targeting lentiviral shRNAs were cotransfected with pHA-APOBEC3(A-H) or pHA-GFP and $pHIV_{NL4\text{-}3\Delta vif}$ expression plasmids at a 1:1 ratio. Forty-eight hours later, viral supernatants were harvested, quantified by $p24^{Gag}$ ELISA, and used to infect the TZM-bl reporter cell line. Transfection of DDX6-depleted HeLa cells consistently resulted in a modest 2- to 4-fold increase in HIV-1 production (see Fig. S5C in the supplemental material). However, depletion of Lsm1 had no effect on virus production (see Fig. S6C in the supplemental material), even though knockdown of both proteins resulted in similar extents of P-body loss (see Fig. S5A and B and S6A and B in the supplemental material). In both cases, P-body depletion had no effect on HIV-1

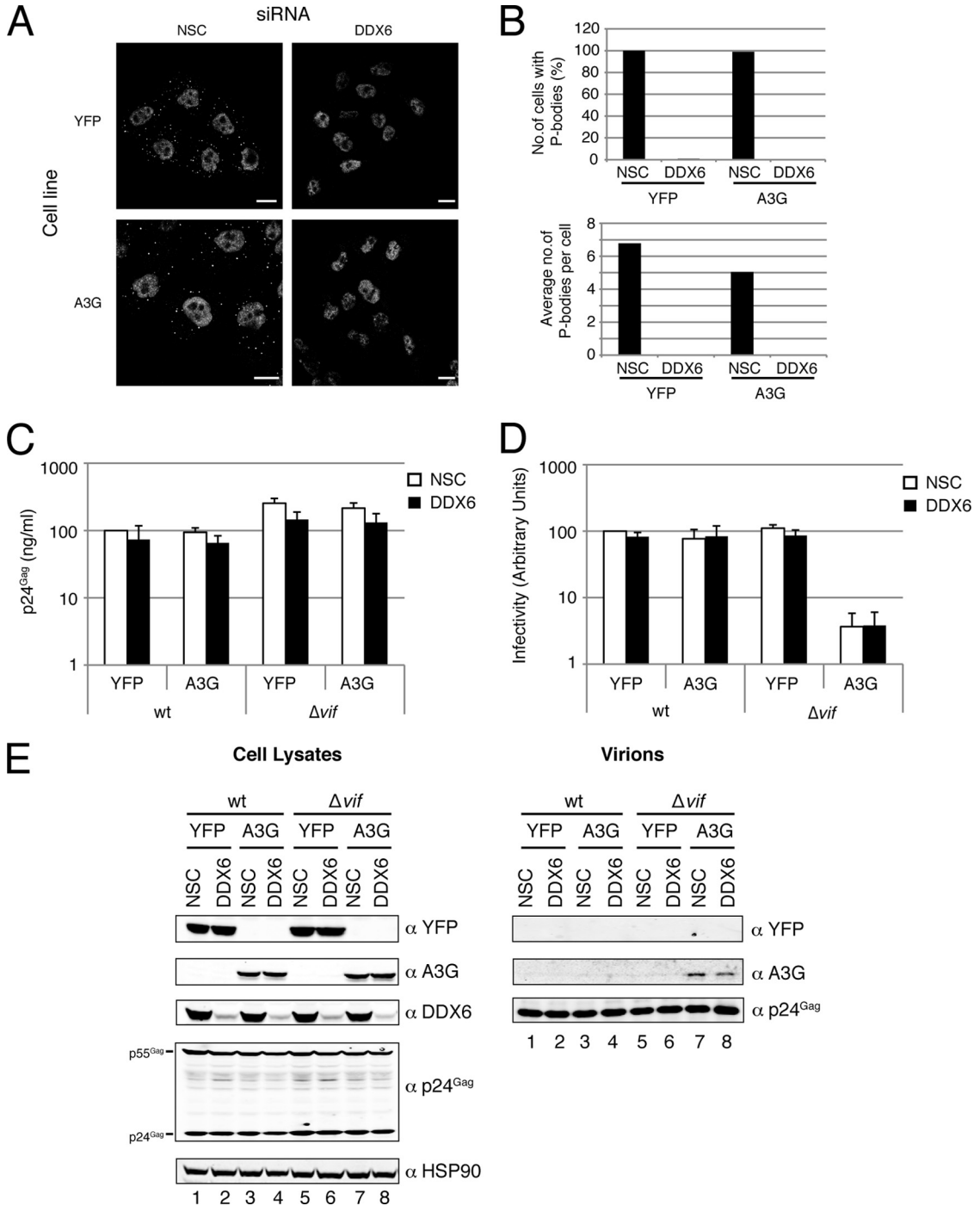

FIG 1 Knockdown of DDX6 does not affect HIV-1 infectious virion production or A3G antiviral activity. (A) HeLa cells stably expressing either A3G or YFP were twice transfected with siRNAs targeting the DDX6 mRNA (DDX6) or a nonsilencing control (NSC). Cells were plated onto coverslips and 24 h later were fixed, permeabilized, and stained with a mouse anti-Ge1 primary antibody and an anti-mouse Alexa Fluor 594-conjugated secondary antibody. Coverslips were mounted onto slides, dried overnight, and imaged using a Leica DM IRE2 confocal microscope. Shown are representative images of immunofluorescence analyses to assess P-body depletion of cells. Bars = 10 μm. (B) Cells were also quantified for the number of cells containing Ge1-marked foci (top) and the average number of these foci per cell (bottom). $n = 100$. (C) Cells, as described for panel A, were infected with VSV-G-pseudotyped HIV_{NL4-3} (wild type [wt]) or $HIV_{NL4-3\Delta vif}$ (Δ*vif*) equivalent to 50 ng $p24^{Gag}$. Forty-eight hours later, supernatants were harvested and quantified by $p24^{Gag}$ ELISA. (D) The infectivity of the virions produced for panel C was assessed by infecting TZM-bl reporter cells with virus equivalent to 5 ng $p24^{Gag}$. For panels C and D, values are normalized to the value for the control siRNA transfected in the YFP-expressing cell line infected with wild-type virus, which is set at 100%. Results are presented as the average of three independent experiments, with error bars denoting the standard deviation. (E) A3G virion incorporation was assessed by purifying virus equivalent to 20 ng $p24^{Gag}$ through a 20% sucrose cushion. Purified virions were lysed and subjected to immunoblotting (right). Lysates from the corresponding producer cells were analyzed in parallel (left).

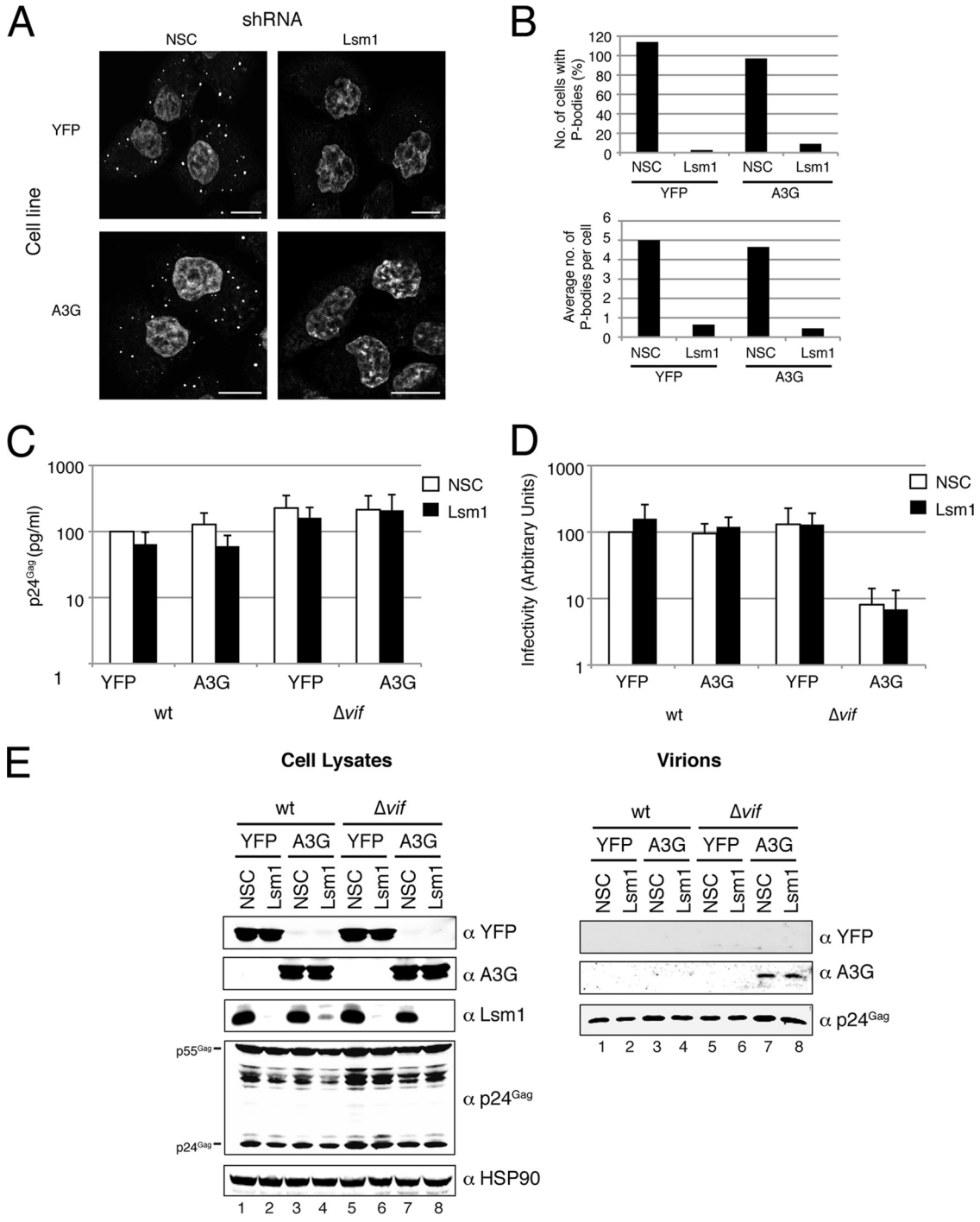

FIG 2 Knockdown of Lsm1 does not affect HIV-1 infectious virion production or A3G antiviral activity. (A) HeLa cells stably expressing either A3G or YFP were transduced with shRNA-encoding vectors targeting the Lsm1 mRNA (Lsm1) or a nonsilencing control (NSC). P-body knockdown was assessed by confocal microscopy as described for Fig. 1A. (B) The number of cells containing Ge1-marked P bodies and the average number of these bodies per cell were quantified as described for Fig. 1B. (C) Cells were infected with wild-type or Δ*vif* virus and analyzed as described for Fig. 1C. (D) The infectivity of the virions produced for panel C was assessed by infecting TZM-bl reporter cells as described for Fig. 1D. (E) A3G virion incorporation was assessed as described for Fig. 1E.

infectivity (with all assays normalized for viral input), APOBEC3 protein antiviral activity, or virion incorporation (see Fig. S5D and E and S6D in the supplemental material), even when the amount of A3G-encoding plasmid DNA was reduced from 1 μg to 0.1 μg (see Fig. S7 in the supplemental material). Based on these observations, we propose that variations in experimental configuration can account for the different conclusions drawn regarding the role of P-body compo-

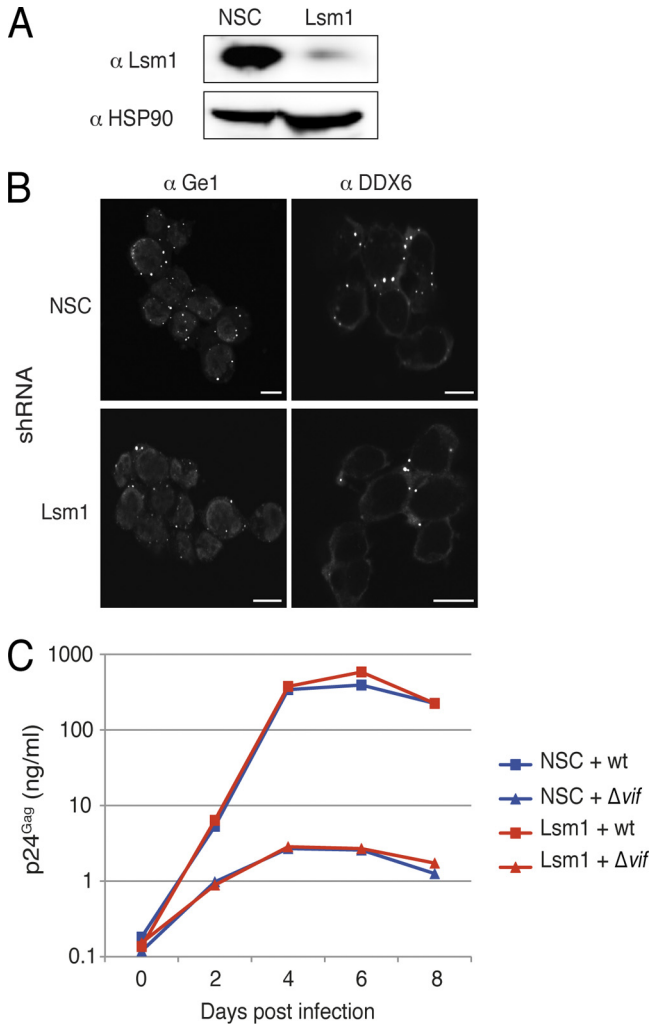

FIG 3 Knockdown of Lsm1 does not affect HIV-1 replication or A3G antiviral activity. (A) Immunoblot analysis of Lsm1 protein levels in HUT78 cells stably transduced with a nonsilencing control (NSC) or Lsm1-targeting (Lsm1) shRNA lentiviral vector. HSP90 is included as a loading control. (B) HUT78 cells, as described for panel A, were plated onto poly-L-lysine-coated coverslips, fixed, and stained with anti-Ge1 and anti-DDX6 primary antibodies and appropriate species-specific Alexa Fluor 594-conjugated secondary antibodies. Samples were imaged by confocal microscopy. Bars = 10 μm. (C) Cells, as described for panel A, were infected with HIV_{NL4-3} (wt) or $HIV_{NL4-3\Delta vif}$ (Δ*vif*) equivalent to 25 ng $p24^{Gag}$. Every 2 days postinfection, supernatants were harvested and analyzed by $p24^{Gag}$ ELISA. A representative result from one of two independent experiments is shown.

nents in HIV-1 production. However, we consider the infection-based methods used for Fig. 1 to 3 to be more reflective of natural HIV-1 replication.

HIV-1 gRNA and Gag do not colocalize with P-body proteins. It has been reported that HIV-1 RNA localizes to P bodies (17, 73). Since we were unable to detect any effect of P-body depletion on HIV-1 replication, we asked whether we could detect viral structural components in P bodies. We constructed an HIV_{NL4-3} provirus containing 24 MS2 binding loops ($pHIV_{NL4-3/24\times MS2}$) and cotransfected it into HeLa cells with pMS2-YFP (Fig. 4A). Importantly, the modified viral RNA is efficiently packaged into virus particles and is able to generate infectious virions comparable to those for an unmodified wild-type control (see Fig. S8 in the supplemental material). MS2-YFP was nuclear in the absence of the HIV-1 proviral construct (35) (Fig. 4A1) but showed a diffuse cytoplasmic distribution in its presence. Unlike a previous report (17), we were unable to observe any localization of gRNA with DDX6-positive P bodies (Fig. 4A2), even when $pHIV_{NL4-3/24\times MS2}$ was titrated down to lower expression levels (see Fig. S9 in the supplemental material). We then determined whether the viral structural protein Gag localized to these foci, which may be anticipated if these are important subcellular packaging domains. To do this, we used a second proviral construct that contained Gag fused to the Venus fluorescent protein ($pHIV_{NL4-3/Gag-Venus}$) (22). There was no apparent colocalization of Gag with P bodies, using either Ge1 or DDX6 as a P-body marker (Fig. 4B). Therefore, we were unable to detect any accumulation of either gRNA or Gag at P bodies.

Role of the Argonaute proteins in HIV-1 infectious virion production and APOBEC3 antiviral activity. There are conflicting reports concerning the effect of depletion of the RISC and P-body component Ago2 on HIV-1 virion production (13, 73). To address the role of the Argonaute protein family in regulating HIV-1 particle production and infectivity, we first depleted each Argonaute protein individually in HeLa cells using siRNAs, which led to a substantial reduction (at least 80%) of each corresponding RNA (Fig. 5A). We then infected these cells with wild-type HIV-1 corresponding to 50 ng $p24^{Gag}$ and measured infectious virion production. Individual depletion of the Argonaute proteins did not significantly affect HIV-1 virion production or infectivity (Fig. 5B and C). As all of the human Argonaute proteins are able to mediate miRNA repression (64, 85, 100) and are thus functionally redundant in this respect, we then attempted to knock down all four proteins simultaneously. We transfected HeLa cells stably transduced with a nonsilencing or Ago4-targeting shRNA with either control siRNA or siRNAs targeting Ago proteins 1, 2, and 3. In the Ago4 shRNA-expressing cell line, Ago1 mRNA expression was reduced by 80%, Ago2 by 60%, Ago3 by 20%, and Ago4 by 50% (Fig. 5D). Importantly, knockdown of the Argonaute proteins either individually or in combination did not affect endogenous P-body formation (Fig. 5E and data not shown). When these cells were challenged with HIV-1, as before, there was a 2-fold decrease in subsequent virion production and a 4-fold increase in the infectivity of the virions produced (Fig. 5F and G). Of note, at this level of Argonaute depletion, there was no overt cell toxicity, but more efficient depletions of the total Argonaute mRNA pool resulted in substantial cell death (data not shown). Therefore, simultaneous depletion of multiple Argonaute proteins can modestly increase HIV-1 infectivity.

To determine if Ago2 is necessary for APOBEC3 antiviral activity, we derived a 293T cell line stably expressing an Ago2 shRNA. Ago2 protein expression was reduced by 85 to 95%, as determined by immunoblotting (see Fig. S10A in the supplemental material), and functional impairment of Ago2 activity was confirmed by using an siRNA targeting the ESCRT (endosomal sorting complex required for transport) component ALIX. RNAi-mediated suppression of endogenous ALIX expression was less efficient in Ago2-depleted 293T cells (see Fig. S10A in the supplemental material). We then cotransfected these cells with $pHIV_{NL4-3\Delta vif}$ and pHA-APOBEC3A, -C, -F, -G, and -H expression plasmids and analyzed virion production and infectivity as before (see Fig. S10B and C in the supplemental

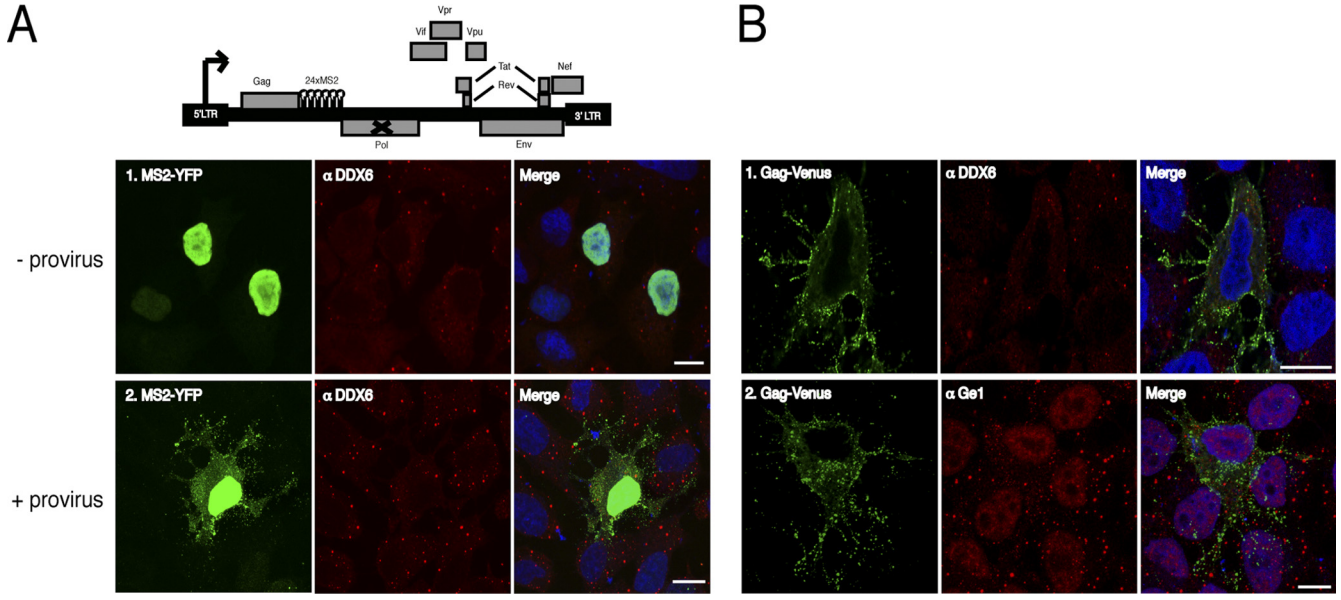

FIG 4 HIV-1 gRNA and Gag do not colocalize with the P-body proteins DDX6 and Ge1. (A) Schematic diagram of the proviral construct containing 24 MS2 binding sites ($pHIV_{NL4\text{-}3/24\times MS2}$) used to visualize HIV-1 genomic RNA. A DNA fragment encoding 24 binding loops from the MS2 bacteriophage RNA was introduced 3′ to the terminus of the *gag* reading frame in an NL4-3 proviral plasmid. Coexpression of an MS2-YFP fusion protein, which binds with high affinity to the MS2 binding loops, allows visualization of the viral RNA. HeLa cells were transfected with either MS2-YFP alone (panel 1) or in combination with $pHIV_{NL4\text{-}3/24\times MS2}$ (panel 2). Cells were fixed at 24 h after transfection and stained with anti-GFP and anti-DDX6 primary antibodies and appropriate species-specific secondary antibodies conjugated to Alexa Fluor 488 or 594. LTR, long terminal repeat. (B) A second NL4-3 proviral construct containing the Venus fluorescent protein fused in frame with Gag ($pHIV_{NL4\text{-}3/Gag\text{-}Venus}$) was transfected into HeLa cells. Twenty-four hours later, the cells were fixed and stained with anti-DDX6 (panel 1) or anti-Ge1 (panel 2) primary antibodies and appropriate species-specific secondary antibodies conjugated to Alexa Fluor 594. For panels A and B, all samples were imaged by confocal microscopy and images are compilations of between 4 and 6 *z* stacks, with merged images presented on the right. Bars = 10 μm.

material). APOBEC3 protein antiviral activity was unperturbed by Ago2 knockdown, even when A3G was expressed at lower levels (see Fig. S10D to F in the supplemental material).

APOBEC3 proteins do not specifically regulate miRNA-mediated translational repression. We next wished to determine the possible role of APOBEC3 proteins in Argonaute activity, specifically, in the regulation of mRNAs through miRNAs. It has been proposed that several APOBEC3 proteins can stimulate cellular gene expression by inhibiting miRNA-mediated repression (46). The Argonaute proteins colocalize with A3G and A3F in P bodies and coimmunoprecipitate in a partially RNase-insensitive manner (36, 37). Therefore, we tested the entire APOBEC3 family for the ability to coimmunoprecipitate with Ago2 using formaldehyde cross-linking. This procedure freezes the RNP complex to prevent dissociation and allows stringent washing to remove proteins that associate nonspecifically (79, 96). Forty-eight hours after 293T cells were cotransfected with pHA-APOBEC3(A-H) and pMyc-Ago2 plasmids, the cells were fixed with 0.05% HCHO, lysed, and sonicated to disrupt insoluble complexes. Ago2 was immunoprecipitated using an anti-Myc antibody and washed, the cross-links were reversed, and proteins were analyzed by immunoblotting (Fig. 6A). In agreement with previously published reports (36, 37, 98), Ago2 efficiently immunoprecipitated A3G and also interacted with A3F and A3H but to lesser extents. Small amounts of A3A and A3C were consistently found to be associated with Ago2, while no detectable interactions were observed for A3B and A3D/E. A3F, A3G, and A3H also coimmunoprecipitated with Ago1 and Ago3 (data not shown). Therefore, unlike localization to P bodies, the ability to interact with Ago2 does not appear to correlate with the packaging efficiencies of the APOBEC3 proteins (see Fig. S2A in the supplemental material).

We then sought to replicate the inhibitory activity of the APOBEC3 proteins on miRNA-mediated repression using established luciferase reporter constructs containing four binding sites for the let-7 miRNA (66). In the absence of any regulatory proteins, expression of luciferase from a construct containing wild-type let-7 binding sites is suppressed by the action of endogenous let-7 compared to that for the mutated control in which all four binding sites are disrupted (Fig. 6B). We cotransfected pHA-GFP and the luciferase reporter constructs and observed a 4- to 5-fold decrease in expression of the wild-type construct, as previously reported (66) (Fig. 6C). Importantly, coexpression of the APOBEC3 proteins generally led to similar changes for the expression of both reporter constructs, implying that the changes observed for the let-7 binding site-containing construct are not due to altered activity of the cognate miRNA. A3C had the most profound effect, enhancing firefly luciferase levels ~10-fold, whereas A3D/E dramatically decreased luciferase expression. Analogous effects were also observed for *Renilla* luciferase, which is commonly used as a transfection control and contains no known miRNA binding sites (Fig. 6D). Our results therefore argue against a role for the APOBEC3 proteins as modulators of miRNA-mediated translational repression but suggest that they could act in other ways to modify gene expression.

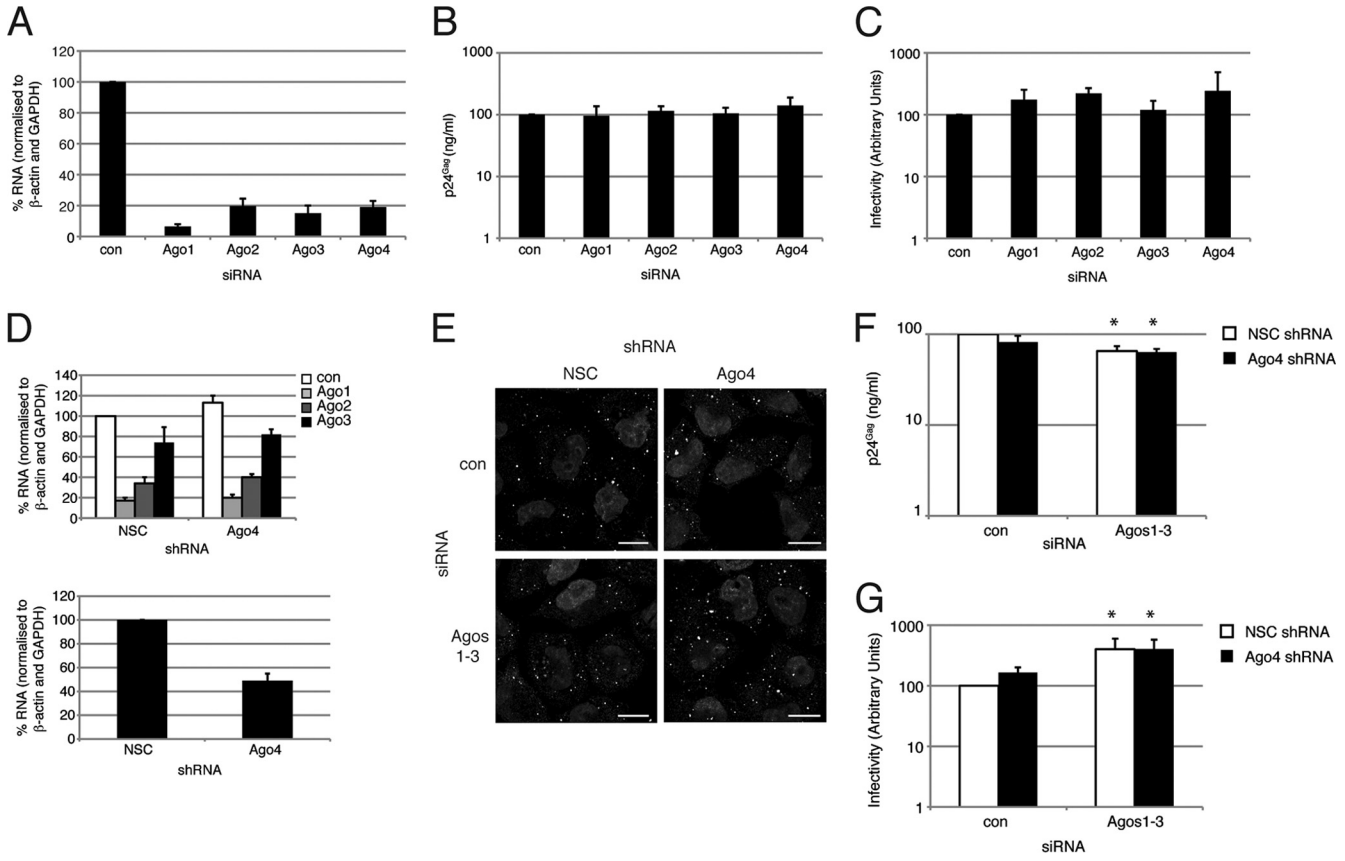

FIG 5 Simultaneous knockdown of Argonaute family members increases HIV-1 infectivity. (A) HeLa cells were twice transfected with siRNAs targeting the Ago proteins 1 to 4 individually, and RNA levels of the Ago transcripts were measured by qPCR. GAPDH, glyceraldehyde-3-phosphate dehydrogenase; con, control. (B) Cells, as described for panel A, were infected with wild-type virus equivalent to 50 ng $p24^{Gag}$. Forty-eight hours later, supernatants were harvested and virus was quantified by $p24^{Gag}$ ELISA. (C) Infectivity of the virions produced for panel B was measured by a TZM-bl reporter assay. (D) HeLa cells stably expressing either a nonsilencing control (NSC) or Ago4-targeting shRNA were twice transfected with equivalent amounts of control siRNA (con) or siRNAs targeting Ago proteins 1, 2, and 3. Cells were harvested, and the RNA levels of the Ago transcripts were measured by qPCR. (E) Cells, as described for panel D, were plated onto coverslips, stained with an anti-DDX6 antibody, and imaged by confocal microscopy. Bars = 10 μm. (F) Cells, as described for panel D, were infected with wild-type virus equivalent to 50 ng $p24^{Gag}$, and virus levels were measured as described for panel B. (G) Infectivity of the virions produced for panel F, measured as described for panel C. For panels B, C, F, and G, values are normalized to the value for the nonsilencing control cell line transfected with control siRNA, which is set at 100%. Results are presented as the average of three independent experiments, with error bars denoting the standard deviation. *, $P < 0.05$ (unpaired two-tailed *t* test).

DISCUSSION

The expansion of the *APOBEC3* family in higher primates, coupled with the fact that the genes themselves are subject to positive selection (87), strongly suggests that APOBEC3 proteins play necessary and fundamental roles in their hosts. The APOBEC3 proteins, along with Trim5α, tetherin, and most recently, SAMHD1, have been identified as host restriction factors that have the intrinsic ability to defend against invading exogenous viruses and endogenous retroelements (45, 58, 75, 90, 92). Although the antiviral activities of the APOBEC3 proteins have been well documented, many questions remain regarding the scope of their functions, potential cellular cofactors, and mechanisms for regulating their protein activity.

Several APOBEC3 proteins localize to P bodies (see Fig. S2 and S3 in the supplemental material), which are RNA-rich microdomains that have previously been reported to influence HIV-1 infectious virion production, positively or negatively (13, 17, 73). However, contrary to these reports, we did not find any substantial effects of P-body depletion or perturbation on HIV-1 infectivity, even when several different experimental approaches were employed (Fig. 1 to 3 and 5). This leads us to conclude that P bodies and at least some P-body components do not appear to regulate HIV-1 replication. It is important to note, however, that although in each experiment protein abundance and, hence, P-body numbers were substantially depleted, without complete elimination of protein expression (e.g., via gene knockout), a role in HIV-1 regulation cannot be comprehensively ruled out. Despite this, with levels of protein depletion comparable to our own, several groups have reported that P-body loss affects HIV-1 production and infectivity (17, 73). The reasons for these disparities are unclear at present, though our own results are consistent across different cell lines, with different experimental configurations, and with altered expression of multiple P-body constituents. In agreement with two reports (17, 73), we did observe a slight increase in virus production upon DDX6 knockdown when employing proviral transfections (see Fig. S5C in the supplemental material). However, this was not observed upon depletion of Lsm1 (see Fig. S6 in the supplemental material), which indicates

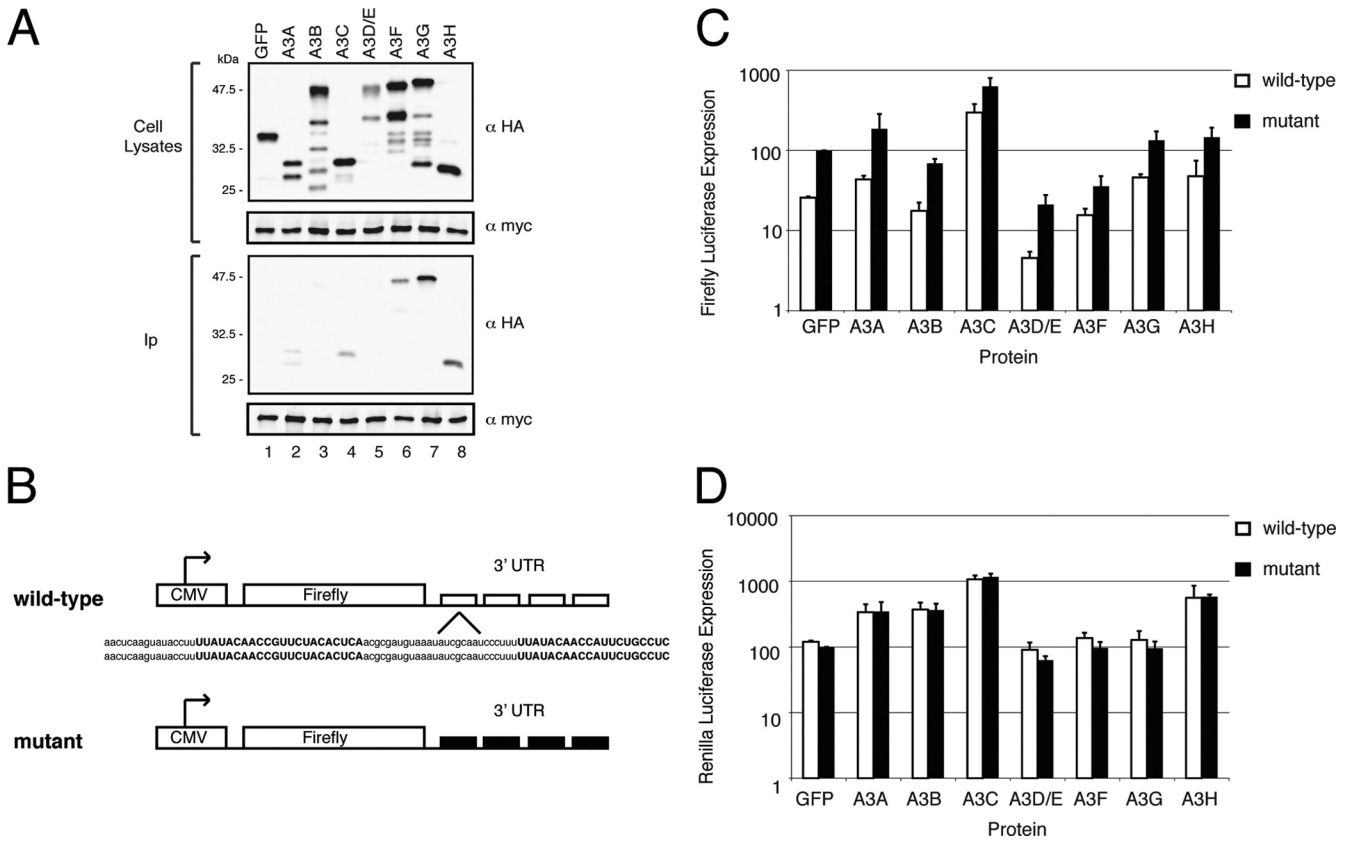

FIG 6 APOBEC3 proteins do not inhibit let-7 miRNA-mediated translational repression. (A) 293T cells cotransfected with equivalent amounts of pHA-GFP or pHA-APOBEC3(A-H) and pMyc-Ago2 expression vectors were incubated with 0.05% formaldehyde, lysed, sonicated, immunoprecipitated (Ip) with an anti-Myc antibody, and then analyzed by immunoblotting using anti-Myc and anti-HA antibodies. A representative result from one of four independent experiments is shown. (B) Schematic diagram of the firefly luciferase reporter constructs used in this study. The wild-type construct contains four binding sites for the let-7 miRNA, while the mutant construct contains mutated binding sites. The sequence of the let-7 binding site is highlighted in bold. CMV, cytomegalovirus; UTR, untranslated region. (C) HeLa cells were cotransfected with pHA-GPF or pHA-APOBEC3(A-H) expression vectors and either the wild-type or mutant firefly luciferase reporter construct as well as a *Renilla* luciferase construct as a transfection control. At 30 h posttransfection, the cells were lysed and a dual-luciferase assay was performed. Raw values of firefly luciferase expression levels are shown. (D) Corresponding raw values of *Renilla* luciferase expression levels from cells as described for panel B. For both panels C and D, values are normalized to the amount of GFP expressed with the mutant reporter, which is set at 100%. Results are presented as the average of four independent experiments, with error bars denoting the standard deviation.

that this modest effect is not due to the general loss of P bodies but is more specifically a consequence of reduced levels of DDX6, a known translational repressor (23). The fact that this was not reproduced using the more physiologically relevant method of infection (Fig. 1 and 2) also questions the possible *in vivo* relevance of this phenomenon.

The role of the Argonaute proteins in modulating HIV-1 virion production is controversial, as depletion of Ago2 has been reported to increase or decrease progeny virion production (13, 73). We individually knocked down each Argonaute protein and did not observe any significant effects on HIV-1 particle production or infectivity (Fig. 5A to C). In order to address potential functional redundancy, we also performed a combined (partial) knockdown of all four Argonaute proteins (Fig. 5D) and found that even though virion production was slightly reduced (Fig. 5F), viral infectivity was modestly increased (Fig. 5G). Because Argonaute depletion did not alter P-body abundance (Fig. 5E), we hypothesize that the Argonaute proteins regulate HIV-1 infectivity by a mechanism which is independent of these foci, perhaps similar to Ago2-mediated regulation of hepatitis C virus replication (9).

Close association of HIV-1 RNA or proteins with P bodies might be expected if the virus was modulated in some manner by these foci. Several reports have shown that HIV-1 RNA and Gag protein localize to P bodies (17, 70, 73). Using an MS2-based tethering system and fluorescently tagged Gag in the context of HIV-1 proviral constructs, we were unable to detect colocalization of HIV-1 gRNA and Gag with DDX6 (Fig. 4), findings consistent with one previous report (14). Therefore, we conclude that HIV-1 gRNA and Gag do not appear to localize to P bodies and the production of infectious virions is not affected when these bodies are disrupted.

It is evident from the work of several groups that certain APOBEC3 proteins interact and colocalize with a diverse array of cellular proteins involved in RNA regulation and metabolism (21, 37, 57, 98). Whether these interactions are necessary for antiviral activity or a different cellular function (or functions) remains to be determined. As the most efficiently packaged APOBEC3 proteins colocalize with DDX6 and Ago2 at P bodies (see Fig. S2 and S3 in the supplemental material), we also sought to determine their influence on APOBEC3 antiviral activity. Using siRNAs and shRNAs targeting DDX6 and Lsm1, respectively, we found that

P-body depletion had no effect on A3G antiviral activity or virion incorporation, for both the ectopically expressed and endogenous protein (Fig. 1 to 3). This was also true for other family members (see Fig. S5 and S6 in the supplemental material) and implies that P bodies are not sites required for the packaging of APOBEC3 proteins into HIV-1 virions.

Although several APOBEC3 proteins interact with Ago2 (Fig. 6A), this protein was not necessary for APOBEC3-mediated viral inhibition (see Fig. S10 in the supplemental material). We also addressed the possibility that the APOBEC3 proteins may be involved in the regulation of Argonaute activity. It has previously been reported that several APOBEC3 proteins inhibit miRNA-mediated repression (46) and A3G specifically inhibits this process through disruption of the interaction between Ago2 and MOV10 (62). However, we found that the APOBEC3 proteins had nonspecific effects on transfected gene expression, as they were able to affect the expression of reporter genes irrespective of miRNA binding sites, indicating that they do not regulate miRNA-mediated translational repression (Fig. 6C and D). We have also recently reported that MOV10 is not required for this cellular process (5). While the basis for this discrepancy is not yet clear, we note that several APOBEC3 family members, particularly A3C, exhibited more general effects on reporter gene expression (Fig. 6C and D). It will be of future interest to identify cellular RNA targets/ligands of the APOBEC3 proteins, as this will focus efforts aimed at understanding the contributions that these proteins may make to RNA regulation and metabolism.

Taken together, our data suggest that P bodies and certain P-body components are not involved in the regulation of APOBEC3 protein antiviral activity or, more generally, HIV-1 replication. However, the Argonaute protein family and miRNAs may contribute to viral regulation. The functional relevance of APOBEC3 colocalization and interaction with numerous P-body proteins therefore remains enigmatic. Provocatively, recent work has implicated the APOBEC3 proteins in causing somatic mutations leading to breast cancer (78). Therefore, it is possible that incorporation into high-molecular-weight ribonucleoprotein complexes and/or P bodies may be mechanisms for regulating APOBEC3 cytidine deaminase activity (21) by sequestering these proteins away from chromosomal DNA.

ACKNOWLEDGMENTS

We thank Eric Freed, Gregory Hannon, Malcolm Martin, Juan Martin-Serrano, Akira Ono, Robert Singer, Joan Steitz, and Wes Sundquist for generously providing reagents and members of the M. H. Malim laboratory for helpful discussions and advice.

This work was supported by grants from the United Kingdom Medical Research Council and the National Institutes of Health (AI070072). N.M.S is a Long-Term Fellow (ALTF 176-2007) of the European Molecular Biology Organization, and C.M.S is a Research Councils United Kingdom Academic Fellow.

REFERENCES

1. **Adachi A, et al.** 1986. Production of acquired immunodeficiency syndrome-associated retrovirus in human and nonhuman cells transfected with an infectious molecular clone. J. Virol. **59**:284–291.
2. **Ahluwalia JK, et al.** 2008. Human cellular microRNA hsa-miR-29a interferes with viral nef protein expression and HIV-1 replication. Retrovirology **5**:117. doi:10.1186/1742-4690-5-117.
3. **Anant S, Davidson NO.** 2000. An AU-rich sequence element (UUUN[A/U]U) downstream of the edited C in apolipoprotein B mRNA is a high-affinity binding site for Apobec-1: binding of Apobec-1 to this motif in the 3′ untranslated region of c-myc increases mRNA stability. Mol. Cell. Biol. **20**:1982–1992.
4. **Anant S, et al.** 2004. Apobec-1 protects intestine from radiation injury through posttranscriptional regulation of cyclooxygenase-2 expression. Gastroenterology **127**:1139–1149.
5. **Arjan-Odedra S, Swanson CM, Sherer NM, Wolinsky SM, Malim MH.** 2012. Endogenous MOV10 inhibits the retrotransposition of endogenous retroelements but not the replication of exogenous retroviruses. Retrovirology **9**:53. doi:10.1186/1742-4690-9-53.
6. **Beckham CJ, et al.** 2007. Interactions between brome mosaic virus RNAs and cytoplasmic processing bodies. J. Virol. **81**:9759–9768.
7. **Beckham CJ, Parker R.** 2008. P bodies, stress granules, and viral life cycles. Cell Host Microbe **3**:206–212.
8. **Beliakova-Bethell N, et al.** 2006. Virus-like particles of the Ty3 retrotransposon assemble in association with P-body components. RNA **12**:94–101.
9. **Berezhna SY, Supekova L, Sever MJ, Schultz PG, Deniz AA.** 2011. Dual regulation of hepatitis C viral RNA by cellular RNAi requires partitioning of Ago2 to lipid droplets and P-bodies. RNA **17**:1831–1845.
10. **Bishop KN, Holmes RK, Malim MH.** 2006. Antiviral potency of APOBEC proteins does not correlate with cytidine deamination. J. Virol. **80**:8450–8458.
11. **Bishop KN, et al.** 2004. Cytidine deamination of retroviral DNA by diverse APOBEC proteins. Curr. Biol. **14**:1392–1396.
12. **Bishop KN, Verma M, Kim EY, Wolinsky SM, Malim MH.** 2008. APOBEC3G inhibits elongation of HIV-1 reverse transcripts. PLoS Pathog. **4**:e1000231. doi:10.1371/journal.ppat.1000231.
13. **Bouttier M, et al.** 2012. Retroviral GAG proteins recruit AGO2 on viral RNAs without affecting RNA accumulation and translation. Nucleic Acids Res. **40**:775–786.
14. **Burnett A, Spearman P.** 2007. APOBEC3G multimers are recruited to the plasma membrane for packaging into human immunodeficiency virus type 1 virus-like particles in an RNA-dependent process requiring the NC basic linker. J. Virol. **81**:5000–5013.
15. **Carlton JG, Agromayor M, Martin-Serrano J.** 2008. Differential requirements for Alix and ESCRT-III in cytokinesis and HIV-1 release. Proc. Natl. Acad. Sci. U. S. A. **105**:10541–10546.
16. **Cen S, et al.** 2004. The interaction between HIV-1 Gag and APOBEC3G. J. Biol. Chem. **279**:33177–33184.
17. **Chable-Bessia C, et al.** 2009. Suppression of HIV-1 replication by microRNA effectors. Retrovirology **6**:26. doi:10.1186/1742-4690-6-26.
18. **Checkley MA, Nagashima K, Lockett SJ, Nyswaner KM, Garfinkel DJ.** 2010. P-body components are required for Ty1 retrotransposition during assembly of retrotransposition-competent virus-like particles. Mol. Cell. Biol. **30**:382–398.
19. **Chester A, et al.** 2003. The apolipoprotein B mRNA editing complex performs a multifunctional cycle and suppresses nonsense-mediated decay. EMBO J. **22**:3971–3982.
20. **Chiu YL, Greene WC.** 2008. The APOBEC3 cytidine deaminases: an innate defensive network opposing exogenous retroviruses and endogenous retroelements. Annu. Rev. Immunol. **26**:317–353.
21. **Chiu YL, et al.** 2006. High-molecular-mass APOBEC3G complexes restrict Alu retrotransposition. Proc. Natl. Acad. Sci. U. S. A. **103**:15588–15593.
22. **Chukkapalli V, Hogue IB, Boyko V, Hu WS, Ono A.** 2008. Interaction between the human immunodeficiency virus type 1 Gag matrix domain and phosphatidylinositol-(4,5)-bisphosphate is essential for efficient gag membrane binding. J. Virol. **82**:2405–2417.
23. **Coller J, Parker R.** 2005. General translational repression by activators of mRNA decapping. Cell **122**:875–886.
24. **Conticello SG, Harris RS, Neuberger MS.** 2003. The Vif protein of HIV triggers degradation of the human antiretroviral DNA deaminase APOBEC3G. Curr. Biol. **13**:2009–2013.
25. **Cougot N, Babajko S, Seraphin B.** 2004. Cytoplasmic foci are sites of mRNA decay in human cells. J. Cell Biol. **165**:31–40.
26. **Cullen BR.** 2006. Role and mechanism of action of the APOBEC3 family of antiretroviral resistance factors. J. Virol. **80**:1067–1076.
27. **Dang Y, et al.** 2008. Human cytidine deaminase APOBEC3H restricts HIV-1 replication. J. Biol. Chem. **283**:11606–11614.
28. **Dang Y, Wang X, Esselman WJ, Zheng YH.** 2006. Identification of APOBEC3DE as another antiretroviral factor from the human APOBEC family. J. Virol. **80**:10522–10533.
29. **Diez J, Ishikawa M, Kaido M, Ahlquist P.** 2000. Identification and

characterization of a host protein required for efficient template selection in viral RNA replication. Proc. Natl. Acad. Sci. U. S. A. **97**:3913–3918.
30. **Dougherty JD, White JP, Lloyd RE.** 2011. Poliovirus-mediated disruption of cytoplasmic processing bodies. J. Virol. **85**:64–75.
31. **Dutko JA, Kenny AE, Gamache ER, Curcio MJ.** 2010. 5′ to 3′ mRNA decay factors colocalize with Ty1 gag and human APOBEC3G and promote Ty1 retrotransposition. J. Virol. **84**:5052–5066.
32. **Fabian MR, Sonenberg N, Filipowicz W.** 2010. Regulation of mRNA translation and stability by microRNAs. Annu. Rev. Biochem. **79**:351–379.
33. **Fisher RD, et al.** 2007. Structural and biochemical studies of ALIX/AIP1 and its role in retrovirus budding. Cell **128**:841–852.
34. **Fouchier RA, Meyer BE, Simon JH, Fischer U, Malim MH.** 1997. HIV-1 infection of non-dividing cells: evidence that the amino-terminal basic region of the viral matrix protein is important for Gag processing but not for post-entry nuclear import. EMBO J. **16**:4531–4539.
35. **Fusco D, et al.** 2003. Single mRNA molecules demonstrate probabilistic movement in living mammalian cells. Curr. Biol. **13**:161–167.
36. **Gallois-Montbrun S, et al.** 2008. Comparison of cellular ribonucleoprotein complexes associated with the APOBEC3F and APOBEC3G antiviral proteins. J. Virol. **82**:5636–5642.
37. **Gallois-Montbrun S, et al.** 2007. Antiviral protein APOBEC3G localizes to ribonucleoprotein complexes found in P bodies and stress granules. J. Virol. **81**:2165–2178.
38. **Goila-Gaur R, Khan MA, Miyagi E, Kao S, Strebel K.** 2007. Targeting APOBEC3A to the viral nucleoprotein complex confers antiviral activity. Retrovirology **4**:61. doi:10.1186/1742-4690-4-61.
39. **Goujon C, Malim MH.** 2010. Characterization of the alpha interferon-induced postentry block to HIV-1 infection in primary human macrophages and T cells. J. Virol. **84**:9254–9266.
40. **Harris RS, et al.** 2003. DNA deamination mediates innate immunity to retroviral infection. Cell **113**:803–809.
41. **Hayes AM, Qian S, Yu L, Boris-Lawrie K.** 2011. Tat RNA silencing suppressor activity contributes to perturbation of lymphocyte miRNA by HIV-1. Retrovirology **8**:36. doi:10.1186/1742-4690-8-36.
42. **Holmes RK, Koning FA, Bishop KN, Malim MH.** 2007. APOBEC3F can inhibit the accumulation of HIV-1 reverse transcription products in the absence of hypermutation. Comparisons with APOBEC3G. J. Biol. Chem. **282**:2587–2595.
43. **Holmes RK, Malim MH, Bishop KN.** 2007. APOBEC-mediated viral restriction: not simply editing? Trends Biochem. Sci. **32**:118–128.
44. **Houzet L, et al.** 2008. MicroRNA profile changes in human immunodeficiency virus type 1 (HIV-1) seropositive individuals. Retrovirology **5**:118. doi:10.1186/1742-4690-5-118.
45. **Hrecka K, et al.** 2011. Vpx relieves inhibition of HIV-1 infection of macrophages mediated by the SAMHD1 protein. Nature **474**:658–661.
45a. **Huang M, Orenstein JM, Martin MA, Freed EO.** 1995. p6Gag is required for particle production from full-length human immunodeficiency virus type 1 molecular clones expressing protease. J. Virol. **69**:6810–6818.
46. **Huang J, et al.** 2007. Derepression of microRNA-mediated protein translation inhibition by apolipoprotein B mRNA-editing enzyme catalytic polypeptide-like 3G (APOBEC3G) and its family members. J. Biol. Chem. **282**:33632–33640.
47. **Huang J, et al.** 2007. Cellular microRNAs contribute to HIV-1 latency in resting primary CD4+ T lymphocytes. Nat. Med. **13**:1241–1247.
48. **Hultquist JF, et al.** 2011. Human and rhesus APOBEC3D, APOBEC3F, APOBEC3G, and APOBEC3H demonstrate a conserved capacity to restrict Vif-deficient HIV-1. J. Virol. **85**:11220–11234.
49. **Huthoff H, Autore F, Gallois-Montbrun S, Fraternali F, Malim MH.** 2009. RNA-dependent oligomerization of APOBEC3G is required for restriction of HIV-1. PLoS Pathog. **5**:e1000330. doi:10.1371/journal.ppat.1000330.
50. **Hutvagner G, Simard MJ.** 2008. Argonaute proteins: key players in RNA silencing. Nat. Rev. Mol. Cell Biol. **9**:22–32.
51. **Iwatani Y, et al.** 2007. Deaminase-independent inhibition of HIV-1 reverse transcription by APOBEC3G. Nucleic Acids Res. **35**:7096–7108.
52. **Jager S, et al.** 2012. Vif hijacks CBF-beta to degrade APOBEC3G and promote HIV-1 infection. Nature **481**:371–375.
53. **Jarmuz A, et al.** 2002. An anthropoid-specific locus of orphan C to U RNA-editing enzymes on chromosome 22. Genomics **79**:285–296.
54. **Jopling CL, Yi M, Lancaster AM, Lemon SM, Sarnow P.** 2005. Modulation of hepatitis C virus RNA abundance by a liver-specific microRNA. Science **309**:1577–1581.
55. **Khan MA, et al.** 2005. Viral RNA is required for the association of APOBEC3G with human immunodeficiency virus type 1 nucleoprotein complexes. J. Virol. **79**:5870–5874.
56. **Klase Z, et al.** 2007. HIV-1 TAR element is processed by Dicer to yield a viral micro-RNA involved in chromatin remodeling of the viral LTR. BMC Mol. Biol. **8**:63.
57. **Kozak SL, Marin M, Rose KM, Bystrom C, Kabat D.** 2006. The anti-HIV-1 editing enzyme APOBEC3G binds HIV-1 RNA and messenger RNAs that shuttle between polysomes and stress granules. J. Biol. Chem. **281**:29105–29119.
58. **Laguette N, et al.** 2011. SAMHD1 is the dendritic- and myeloid-cell-specific HIV-1 restriction factor counteracted by Vpx. Nature **474**:654–657.
59. **Lecellier CH, et al.** 2005. A cellular microRNA mediates antiviral defense in human cells. Science **308**:557–560.
60. **Liddament MT, Brown WL, Schumacher AJ, Harris RS.** 2004. APOBEC3F properties and hypermutation preferences indicate activity against HIV-1 in vivo. Curr. Biol. **14**:1385–1391.
61. **Lin J, Cullen BR.** 2007. Analysis of the interaction of primate retroviruses with the human RNA interference machinery. J. Virol. **81**:12218–12226.
62. **Liu C, et al.** 2012. APOBEC3G inhibits microRNA-mediated repression of translation by interfering with the interaction between Argonaute-2 and MOV10. J. Biol. Chem. **287**:29373–29383.
63. **Liu J, et al.** 2004. Argonaute2 is the catalytic engine of mammalian RNAi. Science **305**:1437–1441.
64. **Liu J, et al.** 2005. A role for the P-body component GW182 in microRNA function. Nat. Cell Biol. **7**:1261–1266.
65. **Lu C, Contreras X, Peterlin BM.** 2011. P bodies inhibit retrotransposition of endogenous intracisternal A particles. J. Virol. **85**:6244–6251.
66. **Lytle JR, Yario TA, Steitz JA.** 2007. Target mRNAs are repressed as efficiently by microRNA-binding sites in the 5′ UTR as in the 3′ UTR. Proc. Natl. Acad. Sci. U. S. A. **104**:9667–9672.
67. **Malim MH.** 2009. APOBEC proteins and intrinsic resistance to HIV-1 infection. Philos. Trans. R. Soc. Lond. B Biol. Sci. **364**:675–687.
68. **Mangeat B, et al.** 2003. Broad antiretroviral defence by human APOBEC3G through lethal editing of nascent reverse transcripts. Nature **424**:99–103.
69. **Mariani R, et al.** 2003. Species-specific exclusion of APOBEC3G from HIV-1 virions by Vif. Cell **114**:21–31.
70. **Martin KL, Johnson M, D'Aquila RT.** 2011. APOBEC3G complexes decrease human immunodeficiency virus type 1 production. J. Virol. **85**:9314–9326.
71. **Mas A, Alves-Rodrigues I, Noueiry A, Ahlquist P, Diez J.** 2006. Host deadenylation-dependent mRNA decapping factors are required for a key step in brome mosaic virus RNA replication. J. Virol. **80**:246–251.
72. **Mehle A, et al.** 2004. Vif overcomes the innate antiviral activity of APOBEC3G by promoting its degradation in the ubiquitin-proteasome pathway. J. Biol. Chem. **279**:7792–7798.
73. **Nathans R, et al.** 2009. Cellular microRNA and P bodies modulate host-HIV-1 interactions. Mol. Cell **34**:696–709.
74. **Navarro F, et al.** 2005. Complementary function of the two catalytic domains of APOBEC3G. Virology **333**:374–386.
75. **Neil SJ, Zang T, Bieniasz PD.** 2008. Tetherin inhibits retrovirus release and is antagonized by HIV-1 Vpu. Nature **451**:425–430.
76. **Newman EN, et al.** 2005. Antiviral function of APOBEC3G can be dissociated from cytidine deaminase activity. Curr. Biol. **15**:166–170.
77. **Niewiadomska AM, et al.** 2007. Differential inhibition of long interspersed element 1 by APOBEC3 does not correlate with high-molecular-mass-complex formation or P-body association. J. Virol. **81**:9577–9583.
78. **Nik-Zainal S, et al.** 2012. Mutational processes molding the genomes of 21 breast cancers. Cell **149**:979–993.
79. **Niranjanakumari S, Lasda E, Brazas R, Garcia-Blanco MA.** 2002. Reversible cross-linking combined with immunoprecipitation to study RNA-protein interactions in vivo. Methods **26**:182–190.
80. **Noueiry AO, Diez J, Falk SP, Chen J, Ahlquist P.** 2003. Yeast Lsm1p-7p/Pat1p deadenylation-dependent mRNA-decapping factors are required for brome mosaic virus genomic RNA translation. Mol. Cell. Biol. **23**:4094–4106.
81. **OhAinle M, Kerns JA, Li MM, Malik HS, Emerman M.** 2008. Antiret-

roelement activity of APOBEC3H was lost twice in recent human evolution. Cell Host Microbe **4**:249–259.
82. **Ouellet DL, et al.** 2008. Identification of functional microRNAs released through asymmetrical processing of HIV-1 TAR element. Nucleic Acids Res. **36**:2353–2365.
83. **Parker R, Song H.** 2004. The enzymes and control of eukaryotic mRNA turnover. Nat. Struct. Mol. Biol. **11**:121–127.
84. **Pfeffer S, et al.** 2005. Identification of microRNAs of the herpesvirus family. Nat. Methods **2**:269–276.
85. **Pillai RS, Artus CG, Filipowicz W.** 2004. Tethering of human Ago proteins to mRNA mimics the miRNA-mediated repression of protein synthesis. RNA **10**:1518–1525.
86. **Reed JC, et al.** 2012. HIV-1 Gag co-opts a cellular complex containing DDX6, a helicase that facilitates capsid assembly. J. Cell Biol. **198**:439–456
87. **Sawyer SL, Emerman M, Malik HS.** 2004. Ancient adaptive evolution of the primate antiviral DNA-editing enzyme APOBEC3G. PLoS Biol. **2**:E275. doi:10.1371/journal.pbio.0020275.
88. **Schafer A, Bogerd HP, Cullen BR.** 2004. Specific packaging of APOBEC3G into HIV-1 virions is mediated by the nucleocapsid domain of the gag polyprotein precursor. Virology **328**:163–168.
89. **Scheller N, et al.** 2009. Translation and replication of hepatitis C virus genomic RNA depends on ancient cellular proteins that control mRNA fates. Proc. Natl. Acad. Sci. U. S. A. **106**:13517–13522.
90. **Sheehy AM, Gaddis NC, Choi JD, Malim MH.** 2002. Isolation of a human gene that inhibits HIV-1 infection and is suppressed by the viral Vif protein. Nature **418**:646–650.
91. **Sheth U, Parker R.** 2003. Decapping and decay of messenger RNA occur in cytoplasmic processing bodies. Science **300**:805–808.
92. **Stremlau M, et al.** 2004. The cytoplasmic body component TRIM5alpha restricts HIV-1 infection in Old World monkeys. Nature **427**:848–853.
93. **Svoboda P, et al.** 2004. RNAi and expression of retrotransposons MuERV-L and IAP in preimplantation mouse embryos. Dev. Biol. **269**:276–285.
94. **Tolia NH, Joshua-Tor L.** 2007. Slicer and the Argonautes. Nat. Chem. Biol. **3**:36–43.
95. **Triboulet R, et al.** 2007. Suppression of microRNA-silencing pathway by HIV-1 during virus replication. Science **315**:1579–1582.
96. **Vasudevan S, Steitz JA.** 2007. AU-rich-element-mediated upregulation of translation by FXR1 and Argonaute 2. Cell **128**:1105–1118.
97. **Wang T, et al.** 2007. 7SL RNA mediates virion packaging of the antiviral cytidine deaminase APOBEC3G. J. Virol. **81**:13112–13124.
98. **Wichroski MJ, Robb GB, Rana TM.** 2006. Human retroviral host restriction factors APOBEC3G and APOBEC3F localize to mRNA processing bodies. PLoS Pathog. **2**:e41. doi:10.1371/journal.ppat.0020041.
99. **Wiegand HL, Doehle BP, Bogerd HP, Cullen BR.** 2004. A second human antiretroviral factor, APOBEC3F, is suppressed by the HIV-1 and HIV-2 Vif proteins. EMBO J. **23**:2451–2458.
100. **Wu L, Fan J, Belasco JG.** 2008. Importance of translation and nonnucleolytic ago proteins for on-target RNA interference. Curr. Biol. **18**:1327–1332.
101. **Yeung ML, et al.** 2005. Changes in microRNA expression profiles in HIV-1-transfected human cells. Retrovirology **2**:81. doi:10.1186/1742-4690-2-81.
102. **Yu Q, et al.** 2004. APOBEC3B and APOBEC3C are potent inhibitors of simian immunodeficiency virus replication. J. Biol. Chem. **279**:53379–53386.
103. **Yu SF, Lujan P, Jackson DL, Emerman M, Linial ML.** 2011. The DEAD-box RNA helicase DDX6 is required for efficient encapsidation of a retroviral genome. PLoS Pathog. **7**:e1002303. doi:10.1371/journal.ppat.1002303.
104. **Yu X, et al.** 2003. Induction of APOBEC3G ubiquitination and degradation by an HIV-1 Vif-Cul5-SCF complex. Science **302**:1056–1060.
105. **Zennou V, Bieniasz PD.** 2006. Comparative analysis of the antiretroviral activity of APOBEC3G and APOBEC3F from primates. Virology **349**:31–40.
106. **Zhang H, et al.** 2003. The cytidine deaminase CEM15 induces hypermutation in newly synthesized HIV-1 DNA. Nature **424**:94–98.
107. **Zhang W, Du J, Evans SL, Yu Y, Yu XF.** 2012. T-cell differentiation factor CBF-beta regulates HIV-1 Vif-mediated evasion of host restriction. Nature **481**:376–379.